CASE FILE COPY

ARR Dec. 1942

NACA-WRL-442

NATIONAL ADVISORY COMMITTEE FOR AERONAUTICS

WARTIME REPORT

ORIGINALLY ISSUED

December 1942 as
Advance Restricted Report

STRENGTH TESTS OF THIN-WALL TRUNCATED CONES OF CIRCULAR SECTION

By Eugene E. Lundquist and Evan H. Schuette

Langley Memorial Aeronautical Laboratory
Langley Field, Va.

REPRODUCED BY
NATIONAL TECHNICAL
INFORMATION SERVICE
U. S. DEPARTMENT OF COMMERCE
SPRINGFIELD, VA. 22161

NACA

WASHINGTON

PRICES SUBJECT TO CHANGE

NACA WARTIME REPORTS are reprints of papers originally issued to provide rapid distribution of advance research results to an authorized group requiring them for the war effort. They were previously held under a security status but are now unclassified. Some of these reports were not technically edited. All have been reproduced without change in order to expedite general distribution.

27

NATIONAL ADVISORY COMMITTEE FOR AERONAUTICS

ADVANCE RESTRICTED REPORT

L-442

STRENGTH TESTS OF THIN-WALL TRUNCATED CONES OF CIRCULAR SECTION

By Eugene E. Lundquist and Evan H. Schuette

SUMMARY

The ends of thin-wall truncated cones of circular section were clamped to rigid bulkheads and the cones subjected to strength tests. The results from torsion tests of five, compression tests of three, and tests in combined transverse shear and bending of 18 truncated cones are given herein. The results of the tests are correlated with the previously published results of corresponding tests of circular cylinders and are presented in charts suitable for use in design.

INTRODUCTION

The strength of thin-wall cylinders has been under investigation by the National Advisory Committee for Aeronautics for a number of years. Previous papers have given the results of various strength tests of thin-wall cylinders of circular and elliptic section.

Because monocoque fuselages usually have some taper, tests were also made to determine the strength of thin-wall truncated cones of circular section in torsion, compression, and combined transverse shear and bending. A preliminary summary of the results is given in reference 1. The present report gives these data in further detail and with greater attention to the conclusions.

MATERIAL

The 17S-T aluminum alloy used in these tests was obtained in sheet form with nominal thicknesses of 0.011, 0.016, and 0.022 inch. The properties of this material

as determined by the National Bureau of Standards from specimens selected at random are given in reference 2. Because all the test cones failed by elastic buckling of the walls at stresses considerably below the yield-point stress, the modulus of elasticity E, which was substantially constant for all sheet thicknesses, is the only property of the material that need be considered. For all sheet material used in these tests, an average value for E of 10.4×10^6 pounds per square inch was used in the analysis of the results.

SPECIMENS

The test specimens were truncated cones 7.5 inches long with end radii of 6.0 and 7.5 inches. (See fig. 1.) The taper of the cones was selected to agree roughly with the taper of a monocoque fuselage. The cones were constructed in the following manner: An aluminum-alloy sheet was first cut to the dimensions of the developed surface. The sheet was then wrapped about and clamped to end bulkheads. When the truncated cone was thus assembled, a butt strap 1 inch wide and of the same thickness as the sheet was fitted, drilled, and bolted in place to close the seam. In the assembly of the specimen, care was taken to avoid having either a looseness of the skin or wrinkles in the walls when finally constructed.

Each of the end bulkheads, to which the loads were applied, was constructed of two steel plates $\frac{1}{4}$ inch thick, separated by a plywood core $1\frac{1}{2}$ inches thick. These parts were bolted together and turned to the specified outside diameter. Steel bands approximately $\frac{1}{4}$ inch thick and machined to the same diameter as the bulkheads were used to clamp the aluminum-alloy sheet to the bulkheads. In order to keep the bands from sliding parallel to the axis of the cone, a tongue and groove was provided between the bulkhead and the band.

APPARATUS AND METHOD

The thickness of each sheet was measured to an estimated precision of ±0.0003 inch at a large number of stations by a dial gage mounted in a special jig. In general, the variation in thickness throughout a given sheet was

not more than 2 percent of the average thickness. The average thicknesses of the sheets were used in all calculations of radius-thickness ratio and stress.

L-442

The loads were applied to the truncated cones with the same apparatus as that used in the corresponding tests of circular cylinders. Descriptions and photographs of the apparatus used in the torsion, compression, and combined transverse shear and bending tests are given in references 2, 3, and 4, respectively.

In all cases loads were applied in increments of 1 percent of the estimated load at failure.

DISCUSSION OF RESULTS

From the photographs of figures 2, 3, and 4, it will be noted that failure always occurs over a large area of the cone wall and not at some particular station between bulkheads. The symbols appearing in figure 4 will be defined later in this report. The properties of the cone and hence the computed stresses for any loading condition vary from point to point along the cone. Thus, in the presentation of the test results for each of the loading conditions considered, a curve is drawn that describes the stress condition throughout the full length of the truncated cone.

Torsion

The shear stress at failure f_s in the plane of the skin at any station is assumed to be given by the formula

$$f_s = \frac{T}{2\pi r^2 t} \tag{1}$$

where

T applied torque at failure

r radius at the particular station

t thickness

At the large end of the cone, where the radius is r_1, the value of f_s is designated f_{s_1}. Then, it follows from equation (1) that

$$f_s = f_{s_1}\left(\frac{r_1}{r}\right)^2 \tag{2}$$

Results of the torsion tests are presented in figure 5, which is the same type of figure as that used by Donnell (reference 5) to present torsion data on circular cylinders. In this figure, μ is Poisson's ratio for the material. The data for each truncated cone tested are represented by a short line that describes the variation of stress along the length of the cone according to equation (2). The results of torsion tests of circular cylinders, taken from reference 2, are also plotted in figure 5.

The lines representing the truncated cones in figure 5 lie across the band of points representing the circular cylinders. The ends of the lines marked with large circles, representing the large ends of the truncated cones, lie approximately along the curve that has been recommended in reference 5 for design of circular cylinders with clamped edges. If the torsional strength of a circular cylinder is assumed to be established by this curve, the shear stress at failure f_{s_1} at the large end of a truncated cone in torsion is equal to the shear stress at failure for a circular cylinder of this radius and of the same length as the truncated cone. The shear stress at failure for any other station along the length of the truncated cone is then given by equation (2).

Compression

The compressive stress at failure f_c, directed along the conical surface, is assumed to be given by

$$f_c = \frac{P}{2\pi rt} \sec \alpha \tag{3}$$

where P is the applied compressive load and α is the angle between the axis of the cone and the longitudinal elements of the surface. At the large end of the cone where the radius is r_1, the value of f_c may be designated f_{c_1}. It then follows from equation (3) that

$$f_c = f_{c_1} \frac{r_1}{r} \tag{4}$$

L-442

Results of the compression tests are presented in figure 6, which is the same type of figure as that used in reference 3 to present compression data on circular cylinders. The data for each truncated cone tested are represented by a short line that describes the variation of stress along the length of the cone according to equation (4). The results of compression tests of circular cylinders, taken from reference 3, are also plotted in figure 6.

The lines representing the truncated cones in figure 6 lie essentially parallel to the band of points representing the circular cylinders. Consequently, if the strength of the truncated cone is to be computed, for purposes of design, on the basis of an equivalent cylinder, either end of the truncated cone may be selected. The assumption that the compressive stress at failure f_{c_1} at the large end of a truncated cone is equal to the compressive stress at failure for a circular cylinder of this radius and the same thickness as the wall of the truncated cone is, however, somewhat conservative. The compressive stress at failure for any other station along the length of the cone is given by equation (4).

Combined Transverse Shear and Bending

The maximum bending stress at failure f_b in the plane of the skin at any station is assumed to be given by the formula

$$f_b = \frac{Mr}{I} \sec \alpha = \frac{M}{\pi r^2 t} \sec \alpha \tag{5}$$

where M is the applied moment at failure and I is the moment of inertia of the cross section at any station, $\pi r^3 t$. The maximum shear stress at failure f_v in the plane of the skin at any station is assumed to be given by the formula

$$f_v = \frac{V' r^2}{I} = \frac{V'}{\pi r t} \tag{6}$$

where

V' effective shear at failure $(V - V_b)$

V applied transverse shear

V_b shear resisted by bending stresses $\frac{M \tan \alpha}{r}$

Equations (5) and (6) are derived in appendix A.

For the analysis and the presentation of data on combined transverse shear and bending, a parameter is desired that is descriptive of a definite loading condition as well as a definite stress condition for the specimen in the same manner that torsion or compression is descriptive of definite loading and stress conditions. Such a parameter is obtained if equation (5) is divided by equation (6). Thus

$$\frac{f_b}{f_v} = \frac{M}{rV'} \sec \alpha \tag{7}$$

The term $\frac{M}{rV'} \sec \alpha$ is, physically, the distance along an element of the cone from the section under investigation to the plane perpendicular to the axis of the cone in which the resultant shear force V acts, expressed in terms of the radius of the cone at the plane of this resultant shear force. In order to show that this interpretation of $\frac{M}{rV'} \sec \alpha$ is correct, reference may be made to figure 7. At station x, the moment $M = V(h-x)$. From the definitions that follow equation (6), $V' = V - \frac{M \tan \alpha}{r}$. Substitution of these values for M and V' in the right-hand side of equation (7) gives

$$\frac{M}{rV'} \sec \alpha = \frac{V(h-x) \sec \alpha}{rV - V(h-x) \tan \alpha} \tag{8}$$

$$= \frac{(h-x) \sec \alpha}{r - (h-x) \tan \alpha} \tag{9}$$

$$= \frac{s}{r_o} \tag{10}$$

Thus, a particular value of $\frac{M}{rV'} \sec \alpha$ is descriptive of a definite loading condition as well as of a definite stress condition. In the analysis of the results of the tests, the variation of the stresses at failure with $\frac{M}{rV'} \sec \alpha$ is studied.

Results of the tests in combined shear and bending are given in figure 8, which is similar to the figure used

L-442

in reference 4 to present data for thin-wall circular cylinders in combined transverse shear and bending. The data for each truncated cone tested are represented by a line that describes the variation of bending stress in terms of the modulus of elasticity E and the ratio t/r along an element of the cone. An inspection of this figure and of the photographs of the types of failure (fig. 4) reveals a transition from a shear type of failure at small values of $\frac{M}{rV'} \sec \alpha$ to a bending type of failure at large values of $\frac{M}{rV'} \sec \alpha$. In the following discussion separate consideration will be given bending failure, shear failure, and the transition from bending to shear failure.

Bending failure (large values of $\frac{M}{rV'} \sec \alpha$).- At large values of $\frac{M}{rV'} \sec \alpha$, failure occurs by a sudden collapse of the outermost compression fibers in the same manner as in the pure-bending tests of circular cylinders reported in reference 6. It is therefore reasonable to suppose that, at these values, the bending strength of a truncated cone should be comparable to the strength of a cylinder of some similar dimensions in pure bending.

For comparison of the present results with the results of the pure-bending tests of circular cylinders reported in reference 6, lines a and b have been drawn on figure 8 representing the upper and lower limits of the strength in pure bending of circular cylinders. These limiting values represent the dispersion of the results of the pure-bending tests of cylinders and were obtained from figure 5 of reference 6. Use of the expression $\frac{f_b}{E} \frac{r}{t}$ as ordinate in figure 8 makes the location of the limiting lines a and b independent of r/t, provided the maximum bending stress at failure in pure bending is given by an equation of the type

$$S_b = kE \frac{t}{r} \tag{11}$$

where k is a coefficient, the variation of which describes the scatter of test data. The lines a and b in figure 8 simply represent the limiting values of this coefficient.

Equation (11) may be considered valid over the small range of values of r/t represented by the truncated cones tested. Hence the lines a and b should represent reasonably well the conditions for bending failure over the full length of a truncated cone. The condition of pure bending for a truncated cone is, from considerations of internal stresses ($V' = 0$), given by a transverse shear force V located at the apex of the cone. Figure 8 shows that the test results represented by the bending-stress diagrams lie between lines a and b at large values of $\frac{M}{rV'} \sec \alpha$.

Shear failure (small values of $\frac{M}{rV'} \sec \alpha$).- At small values of $\frac{M}{rV'} \sec \alpha$, failure occurs in shear by the formation of diagonal shear wrinkles on the sides of the cones. (See fig. 4.) It is therefore reasonable to suppose that, at these values, the shear strength of a thin-wall truncated cone should be closely related to the strength of a truncated cone of the same dimensions in torsion (pure shear).

For comparison with the results of the torsion tests included in the present paper, lines c and d have been drawn in figure 8 representing the strength in pure shear for the small and for the large ends of a cone, respectively. These lines were obtained by plotting the equation

$$\frac{f_b}{E} \frac{r}{t} = \frac{S_s}{E} \frac{r}{t} \frac{M}{rV'} \sec \alpha \qquad (12)$$

Equation (12) is obtained from equation (7) by transposing terms, multiplying by $\frac{1}{E} \frac{r}{t}$, and substituting S_s for f_v, where S_s is the shear stress at failure for a truncated cone of the same dimensions in torsion. The lines c and d in figure 8 represent the values of $\frac{S_s}{E} \frac{r}{t}$ determined from figure 5 for the two ends of the truncated cones of the same thickness as the cones tested in combined transverse shear and bending.

For low values of $\frac{M}{rV'} \sec \alpha$, the bending-stress diagrams lie above lines c and d. This fact indicates that the transverse shear stress on the neutral axis at

L-442

failure is higher than the shear stress at failure in torsion. The relation determined for circular cylinders in combined transverse shear and bending (reference 4) can be used to take account of this difference. If S_v is the shear stress on the neutral axis at failure in pure transverse shear and S_s is the shear stress at failure for a cone of the same dimensions in torsion, S_v and S_s may be related by the approximate equation

$$S_v = 1.25\ S_s \tag{13}$$

Transition from shear to bending failure (intermediate values of $\frac{M}{rV'}$ sec α).- Figures 4 and 8 reveal that the transition from shear to bending failure is not so abrupt as the intersections of lines a with c and b with d indicate. At the intermediate values of $\frac{M}{rV'}$ sec α, the transition from failure by shear to failure by bending is accompanied by a reduction in strength that is of the same order of magnitude as the corresponding reduction for thin-wall cylinders in combined transverse shear and bending. (See reference 4.) An analysis similar to that used for thin-wall cylinders reveals that the design chart presented in figure 8 of reference 4 also applies to thin-wall truncated cones in combined transverse shear and bending if $\frac{M}{rV}$ is replaced by $\frac{M}{rV'}$ sec α. This design chart is presented in figure 9 of the present report.

In figure 8 the two lines e and f were obtained from figure 9, in one case the value of $\frac{S_b}{S_v}$ corresponding to lines a and c being used and in the other case the value of $\frac{S_b}{S_v}$ corresponding to lines b and d. Inspection of the figure indicates that these two curves represent reasonably well the limits of the experimental data plotted.

In order to use the curves of figure 9 in design, it is necessary to know the loading condition $\frac{M}{rV'}$ sec α and to be able to predict the values of S_v and S_b for the

cone. The value of $\frac{M}{rV'}$ sec α is established by the dimensions of the truncated cone and the external loads. The allowable stress in transverse shear S_v depends upon the allowable stress in torsion, that is, pure shear, according to equation (13). In the absence of test data on the strength of truncated cones in pure bending, the value of S_b to be used should be based upon test data for thin-wall cylinders of comparable r/t ratio in pure bending. Such data are contained in reference 6. These data scatter widely and some judgment must therefore be exercised in the selection of a value for S_b.

If the three quantities $\frac{M}{rV'}$ sec α, S_v, and S_b are known, the maximum allowable moment or the bending stress on the extreme fiber can be read from the chart of figure 9 as a percentage of the value for pure bending. The strength in shear, then, need not be investigated because its effect has been taken into account by a reduced bending strength.

When the strength of any section between adjacent bulkheads is to be checked, the largest absolute value of $\frac{M}{rV'}$ sec α should be used to enter the chart of figure 9 whenever $\frac{M}{rV'}$ sec α lies between $-\csc\alpha$ and $+\infty$. For values of $\frac{M}{rV'}$ sec α between $-\csc\alpha$ and $-\infty$, the lowest absolute value should be used. This procedure gives conservative values and may be verified from appendix B.

CONCLUSIONS

The strength of thin-wall truncated cones may be computed by the formulas used for thin-wall cylinders, if proper account is taken of the angle α between the elements and the axis of the cone. For cylinders, $\alpha = 0$. In the tests reported herein, $\alpha = \tan^{-1}(\frac{1}{5})$. The following conclusions may therefore be considered valid provided that α does not exceed $\tan^{-1}(\frac{1}{5})$:

<u>Torsion.</u>- For torsion, the shear stress f_s in the plane of the skin at any station is given by the formula

$$f_s = \frac{T}{2\pi r^2 t}$$

where

L-442

T applied torque

r radius at the particular station

t thickness

The shear stress at failure f_{s_1} at the large end of a truncated cone in torsion is equal to the shear stress at failure for a circular cylinder of this radius and the same length as the truncated cone. The shear stress at failure for any other station along the length of the truncated cone is given by the formula

$$f_s = f_{s_1}\left(\frac{r_1}{r}\right)^2$$

where r_1 is the radius at the large end of the cone.

Compression.- On the assumption that the internal compressive stress f_c acts in the direction of the element,

$$f_c = \frac{P}{2\pi r t} \sec \alpha$$

where P is the applied compressive load. The compressive stress at failure f_{c_1} at the large end of a truncated cone is equal to the compressive stress at failure for a circular cylinder of this radius and of the same thickness as the wall of the truncated cone. The compressive stress at failure for any other station along the length of the cone is given by the formula

$$f_c = f_{c_1} \frac{r_1}{r}$$

Combined transverse shear and bending.- If the bending stresses are assumed to act in the direction of the elements, a portion of the transverse shear V is resisted by the bending stresses. A moment M on a truncated cone of circular cross section reduces the shear by an amount V_b where

$$V_b = \frac{M \tan \alpha}{r}$$

In combined transverse shear and bending, the effective shear V' is, therefore,

$$V' = V - V_b$$

The effective transverse shear causes a shear stress f_v in the plane of the skin at the neutral axis that is given by the formula

$$f_v = \frac{V'}{\pi r t}$$

The bending stress f_b in the plane of the skin at any station is given by the formula

$$f_b = \frac{M}{\pi r^2 t} \sec \alpha$$

For large values of $\frac{M}{rV'} \sec \alpha$, failure occurs in bending. For small values of $\frac{M}{rV'} \sec \alpha$, failure occurs in shear. For intermediate values of $\frac{M}{rV'} \sec \alpha$, the failure is a combination of shear and bending. The allowable strength in combined transverse shear and bending is given by a design chart similar to that previously published for thin-wall circular cylinders.

Langley Memorial Aeronautical Laboratory,
National Advisory Committee for Aeronautics,
Langley Field, Va.

APPENDIX A

BENDING AND SHEAR STRESSES IN A CONE

The relations between the internal stress and the applied forces in a tapered beam are slightly different from the corresponding relations for a uniform beam. In this appendix, formulas for the bending and shearing stresses due to the application of a single transverse force on a hollow circular cone are derived.

L-442

Figure 10 shows a truncated cone of constant wall thickness with the large end fixed in position and with a transverse force V applied at the small end. At any typical station, the mean radius of the cone is r.

The assumptions are:

1. Bending stresses are directed along the surface of the cone toward the apex

2. Bending stresses are proportional to the distance from the neutral axis, as in the ordinary theory of bending

3. Shear stresses are directed parallel to the surface of the cone

Bending stresses.- An element of area of the cross section $rt\,d\theta$ located at an angle θ measured from the neutral axis, as shown in figure 10, is considered. By assumption 2, the stress on the element is $f_b \sin\theta$, where f_b is the stress on the extreme fiber. The force dF on this element is, therefore,

$$dF = (f_b \sin\theta)\, rt\, d\theta \tag{A1}$$

The moment of dF about the neutral axis is

$$dM = (\cos\alpha)(r \sin\theta)(f_b \sin\theta)\, rt\, d\theta \tag{A2}$$

The total moment M is obtained by integration around the circumference of the cone. Thus,

$$M = f_b r^2 t \cos\alpha \int_0^{2\pi} \sin^2\theta \; d\theta$$

$$= f_b \pi r^2 t \cos\alpha \tag{A3}$$

Thus, the bending stress f_b at the extreme fiber in terms of the applied bending moment M is

$$f_b = \frac{M}{\pi r^2 t \cos\alpha} = \frac{Mr}{I} \sec\alpha \tag{A4}$$

where I is the moment of inertia of the cross section at any station and equals $\pi r^3 t$.

Shear stresses.- From the assumption that the bending stresses are directed along the surface of the cone toward the apex, it follows that the bending stresses have a component in the direction of the shear force V. This component resists a part of the shear force V and therefore reduces the shear stresses.

The shear force resisted by the bending force dF in an element of the cone is

$$dV_b = (\sin\alpha \sin\theta)\, dF$$

$$= (\sin\alpha \sin\theta)(f_b \sin\theta)\, rt\, d\theta \qquad \text{(A5)}$$

The total shear resisted by the bending stresses is obtained by integration around the circumference of the cone. Thus,

$$V_b = f_b\, rt \sin\alpha \int_0^{2\pi} \sin^2\theta\, d\theta$$

$$= f_b\, \pi rt \sin\alpha \qquad \text{(A6)}$$

Substitution of the value of f_b from equation (A4) in equation (A6) gives

$$V_b = \frac{M \tan\alpha}{r} \qquad \text{(A7)}$$

The effective shear V' that causes shear stresses in the walls of the cone is therefore the total applied shear V minus the shear resisted by the bending stresses V_b; that is,

$$V' = V - V_b \qquad \text{(A8)}$$

In order to determine the shear stresses in a cone, the part element of a cone shown in figure 11 is considered. The x-components of the forces due to bending are, at station x,

$$(F_b)_x = \int_\theta^{\pi/2} f_b \sin\theta \cos\alpha\, rt\, d\theta \qquad \text{(A9)}$$

and, at station $x + dx$,

L-442

$$(F_b)_{x+dx} = \int_{\theta}^{\pi/2} \left(f_b + \frac{df_b}{dx}\,dx\right) \sin\theta \cos\alpha \left(r + \frac{dr}{dx}\,dx\right) t\, d\theta \tag{A10}$$

By virtue of symmetry the shear stress at the extreme fiber is zero. The x-component of force due to shear is therefore

$$(F_v)_\theta = (f_v)_\theta\, t\, (dx \sec\alpha) \cos\alpha \tag{A11}$$

The equation of equilibrium for the forces in the x-direction is therefore, if terms of higher order are neglected,

$$(f_v)_\theta \sec\alpha + \int_{\theta}^{\pi/2} \frac{df_b}{dx} \sin\theta\, r\, d\theta + \int_{\theta}^{\pi/2} f_b \sin\theta \frac{dr}{dx}\, d\theta = 0 \tag{A12}$$

from which

$$(f_v)_\theta = -\cos\alpha \cos\theta \left(r \frac{df_b}{dx} + f_b \frac{dr}{dx}\right) \tag{A13}$$

By differentiation of equation (A4),

$$\frac{df_b}{dx} = \frac{\frac{dM}{dx}}{\pi r^2 t \cos\alpha} - \frac{2M \frac{dr}{dx}}{\pi r^3 t \cos\alpha} \tag{A14}$$

At station x, the moment $M = V(h - x)$. Therefore

$$\frac{dM}{dx} = -V \tag{A15}$$

Also

$$\frac{dr}{dx} = -\tan\alpha \tag{A16}$$

Substitution of equations (A14), (A15), and (A16) in equation (A13) gives

$$(f_v)_\theta = \left(\frac{V}{\pi r t} - \frac{M \tan\alpha}{\pi r^2 t}\right) \cos\theta$$

$$= \frac{V'}{\pi r t} \cos\theta \tag{A17}$$

The maximum shear stress f_v, which occurs at the neutral axis, is given by the formula

$$f_v = \frac{V'}{\pi r t} = \frac{V' r^2}{I} \tag{A18}$$

APPENDIX B

EFFECT OF VARIATION IN THE POINT OF APPLICATION OF THE SHEAR FORCE ON THE BENDING STRESSES IN A CONE

Bending-stress diagrams for cones in combined transverse shear and bending for which the value of $\frac{M}{rV'} \sec \alpha$ is positive are shown in figure 8. Reference to figure 7 and equation (10) shows, however, that the quantity $\frac{M}{rV'} \sec \alpha$ can also have negative values. These negative values occur when the resultant shear force V is located either to the right of the apex of the cone (negative r_o) or to the left of station x, the section at which bending stress is determined (negative s).

A diagram similar to that of figure 8 but including the negative values of $\frac{M}{rV'} \sec \alpha$ is shown in figure 12. A few hypothetical bending-stress diagrams for cones of the type studied in this paper are plotted in figure 12 to indicate their shapes. The boundary lines correspond to the two lines e and f used in figure 8 to represent the scatter of test data.

Three distinct regions can be defined in figure 12. The region in which $\frac{M}{rV'} \sec \alpha$ varies from 0 to $+\infty$ is the same as that shown in figure 8 and corresponds to a variation in the location of the resultant shear force from station x to the apex of the cone. As the shear force moves from the apex out to infinity on the right,

L-442

$\frac{M}{rV'}$ sec α varies from $-\infty$ to a value of $-\csc\alpha$ (in this case, -5.1) and defines the left-hand region of figure 12, in which the bending stresses are shown as positive. As the shear force moves to the left from station x to infinity, $\frac{M}{rV'}$ sec α varies from 0 to $-\csc\alpha$ and defines the region in figure 12 in which the bending stresses are shown as negative. The pure-bending condition, for which the effective shear V' is equal to zero, is obtained by placing the resultant shear force V at the apex of the cone; that is, $\frac{M}{rV'}\sec\alpha = \pm\infty$.

REFERENCES

1. Anon.: Strength of Aircraft Elements. ANC-5 Army-Navy-Civil Committee on Aircraft Requirements. U.S. Govt. Printing Office, Oct. 1940.

2. Lundquist, Eugene E.: Strength Tests on Thin-Walled Duralumin Cylinders in Torsion. T.N. No. 427, NACA, 1932.

3. Lundquist, Eugene E.: Strength Tests of Thin-Walled Duralumin Cylinders in Compression. Rep. No. 473, NACA, 1933.

4. Lundquist, Eugene E.: Strength Tests of Thin-Walled Duralumin Cylinders in Combined Transverse Shear and Bending. T.N. No. 523, NACA, 1935.

5. Donnell, L. H.: Stability of Thin-Walled Tubes under Torsion. Rep. No. 479, NACA, 1933.

6. Lundquist, Eugene E.: Strength Tests of Thin-Walled Duralumin Cylinders in Pure Bending. T.N. No. 479, NACA, 1933.

L-442

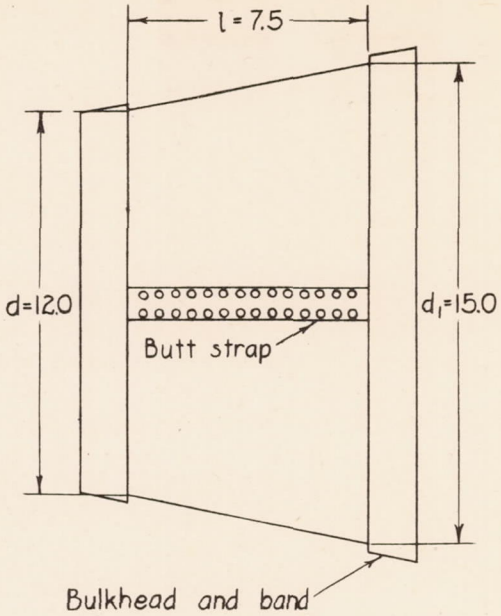

Figure 1.- Side view of test specimen.

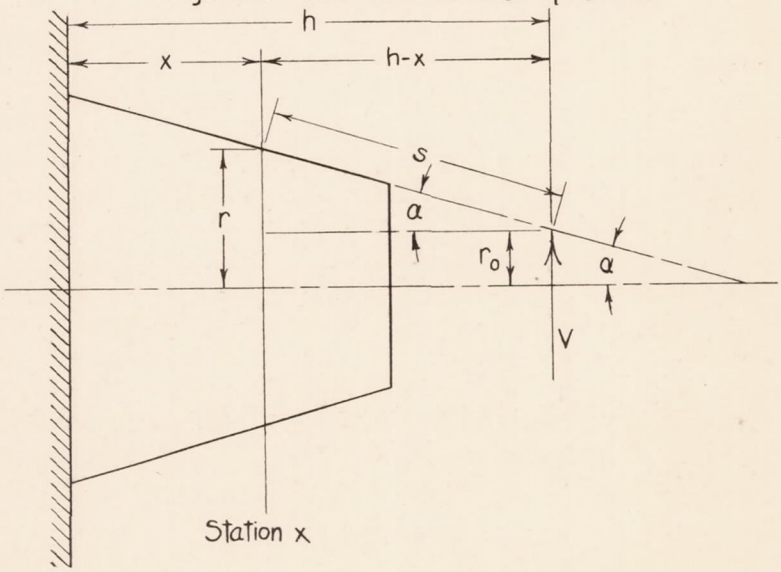

Figure 7.- Sketch of cone and resultant shear force.

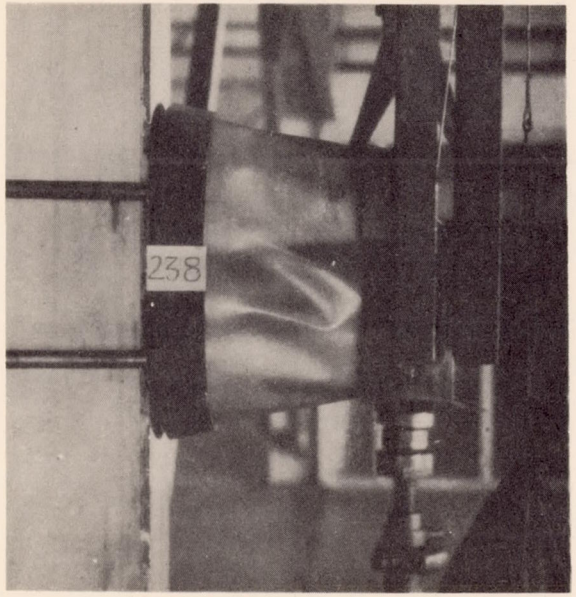

Figure 2. - Truncated cone after failure in torsion.

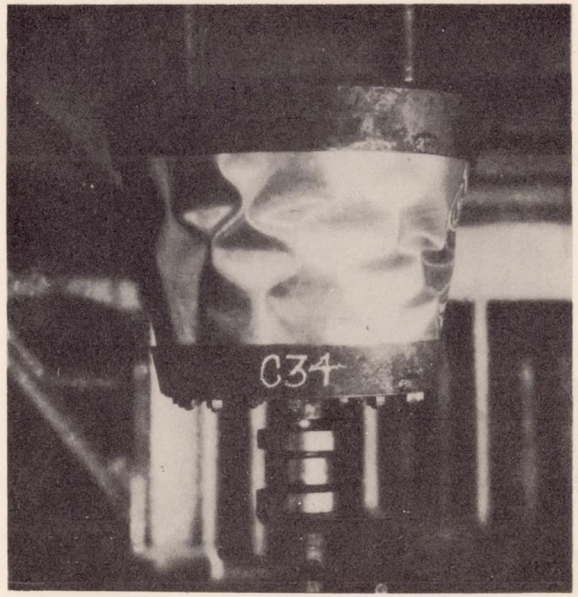

Figure 3. - Truncated cone after failure in compression.

L-442

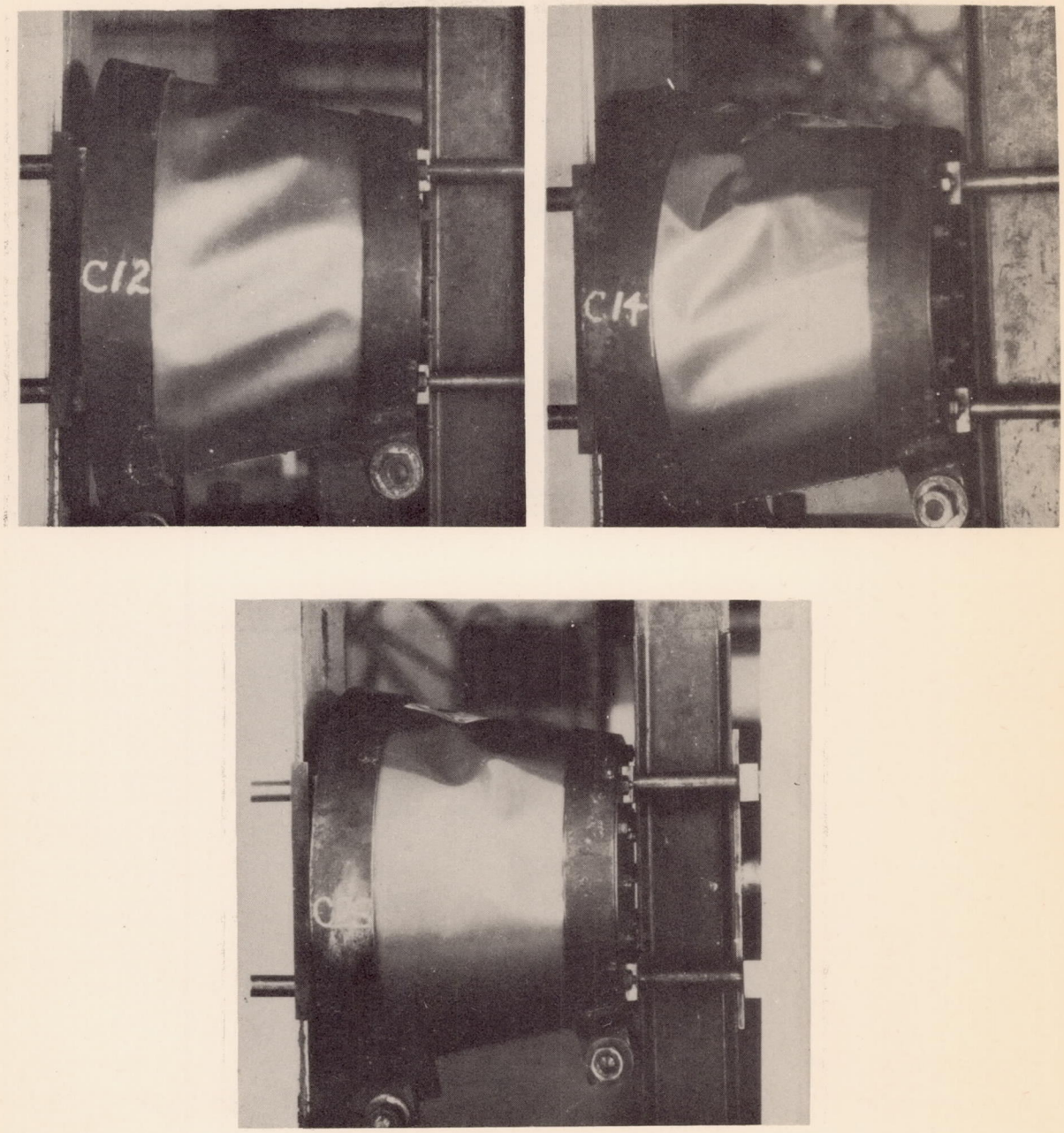

Figure 4.- Truncated cones after failure in combined transverse shear and bending, showing transition from shear to bending failure as $(M/rV')\sec\alpha$ varies from small to large values.

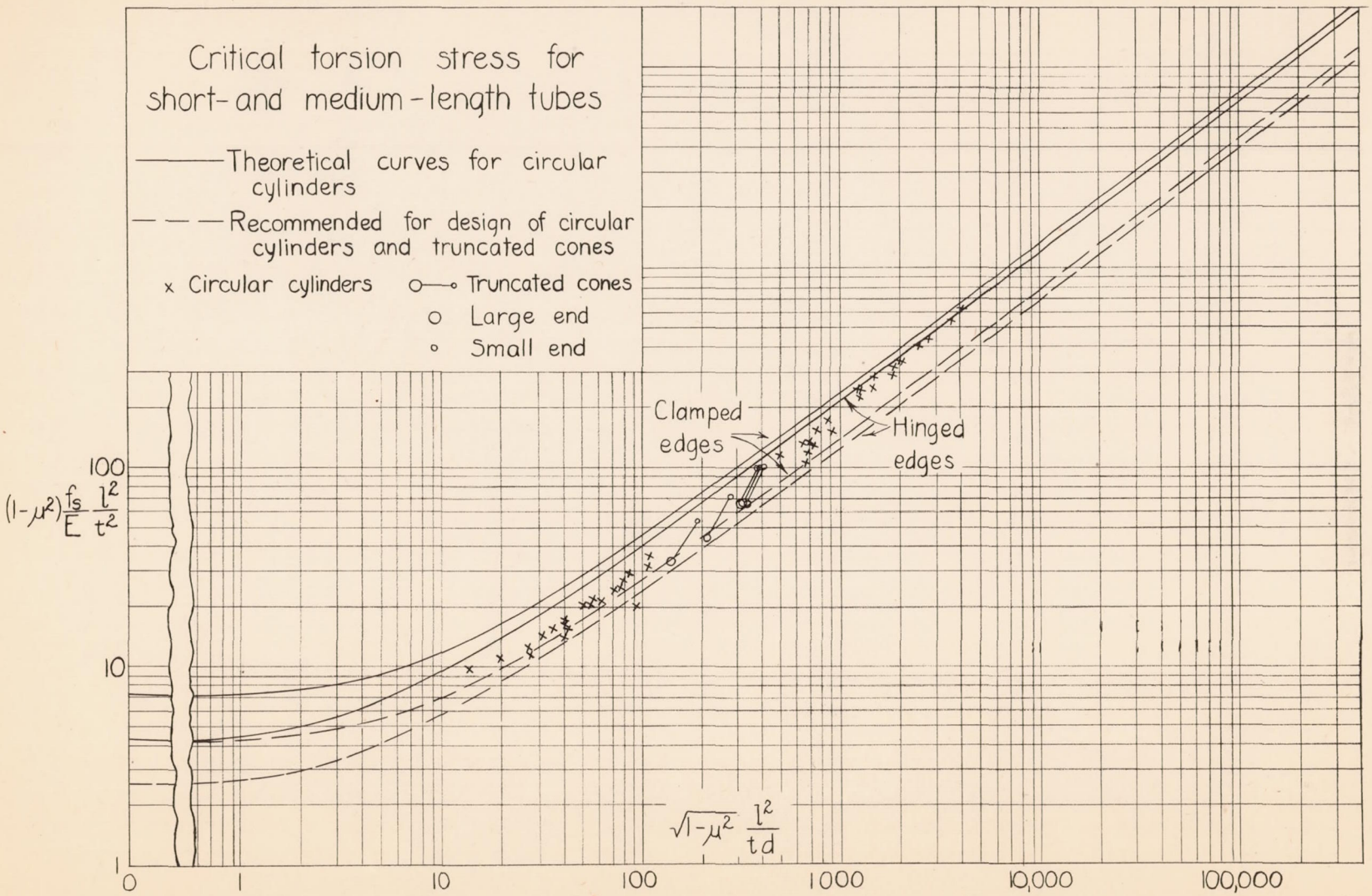

Figure 5. - Shear stress at failure f_s for truncated cones in torsion. (See fig. 1, reference 5; data for circular cylinders from reference 2.)

L-442

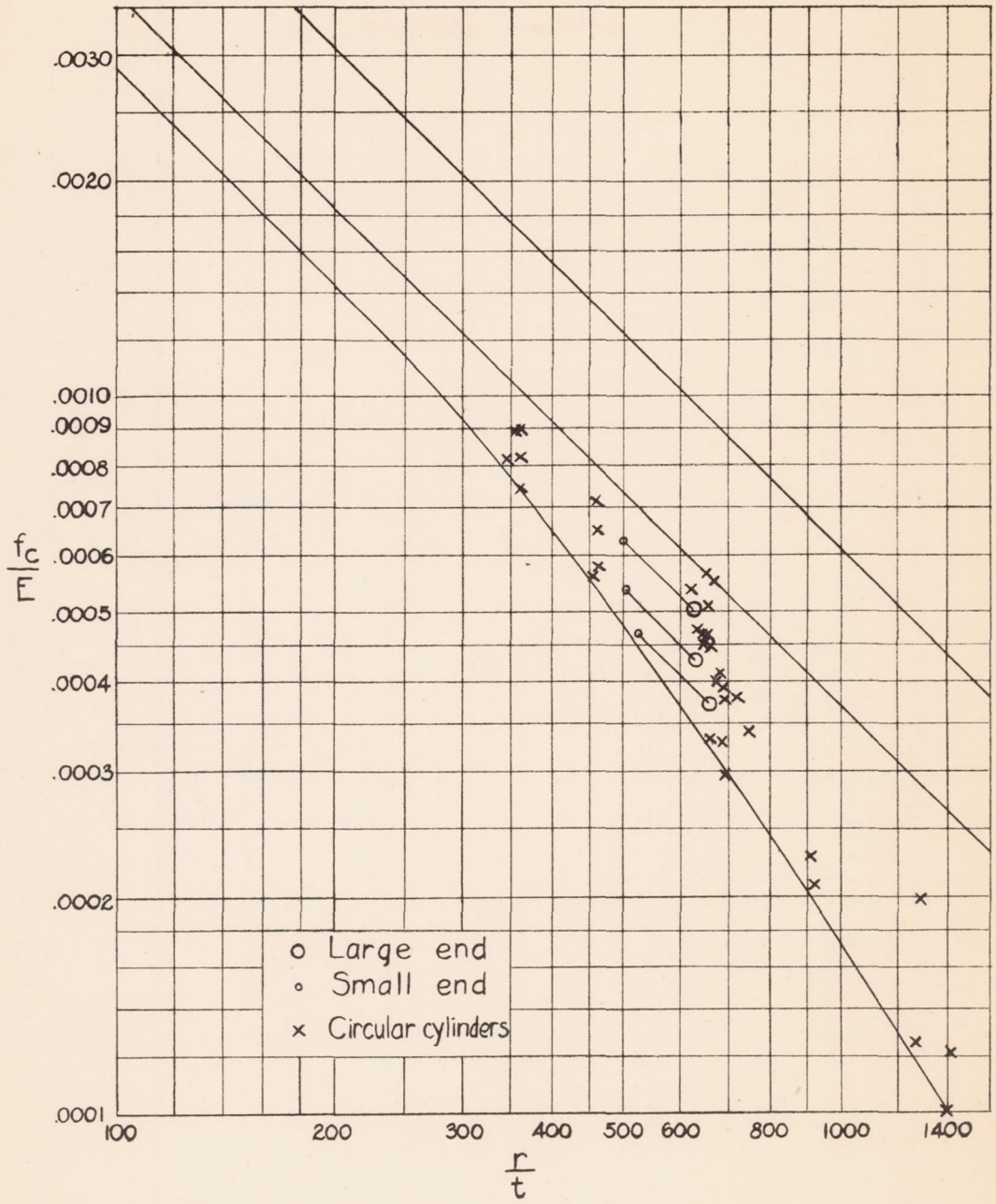

Figure 6.- Plot of f_c/E against r/t for truncated cones in compression. (Data for circular cylinders obtained from reference 3.)

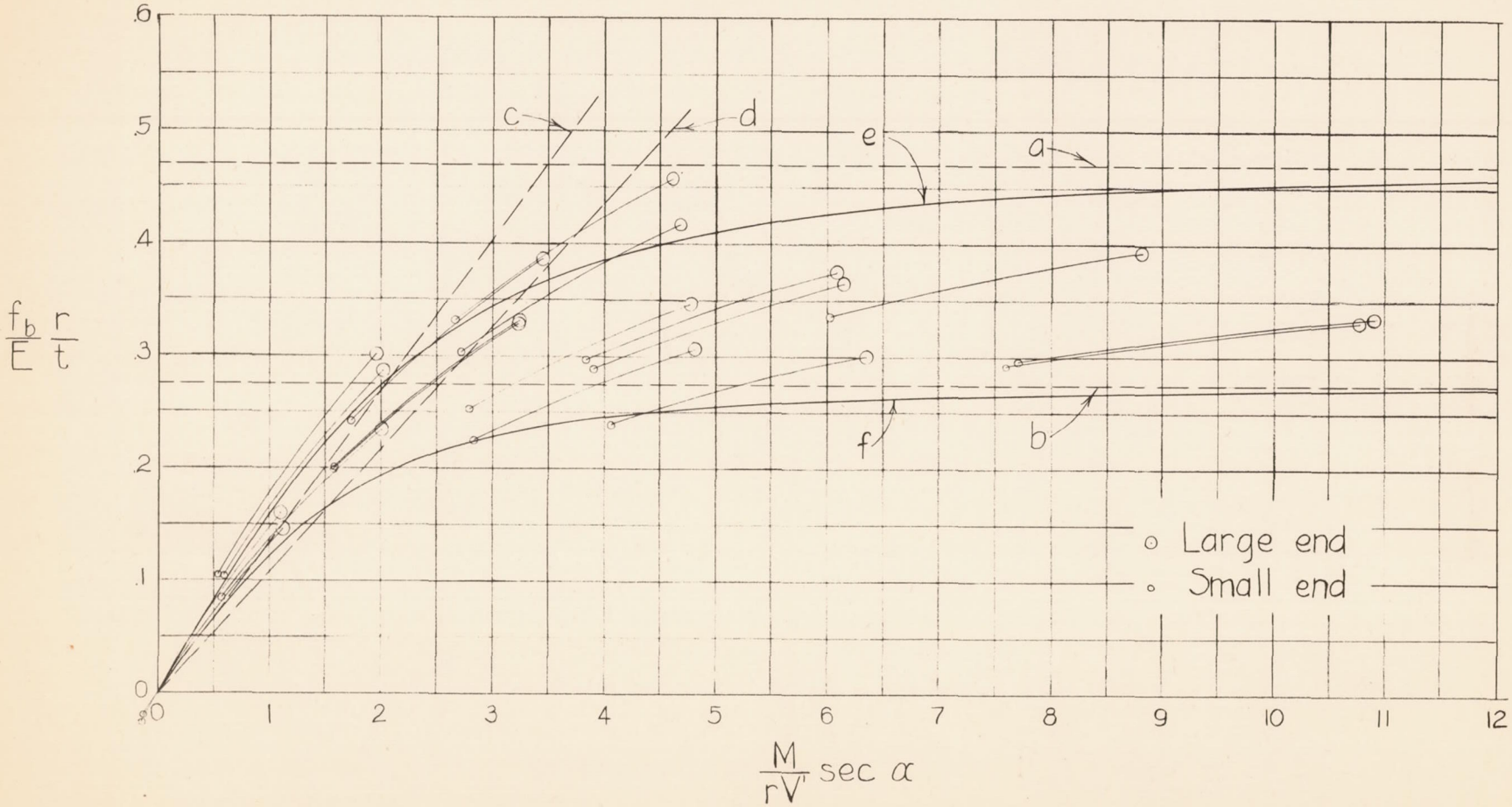

Figure 8.- Bending-stress diagrams for truncated cones in combined transverse shear and bending. (Lines a and b obtained from fig. 5, reference 6.)

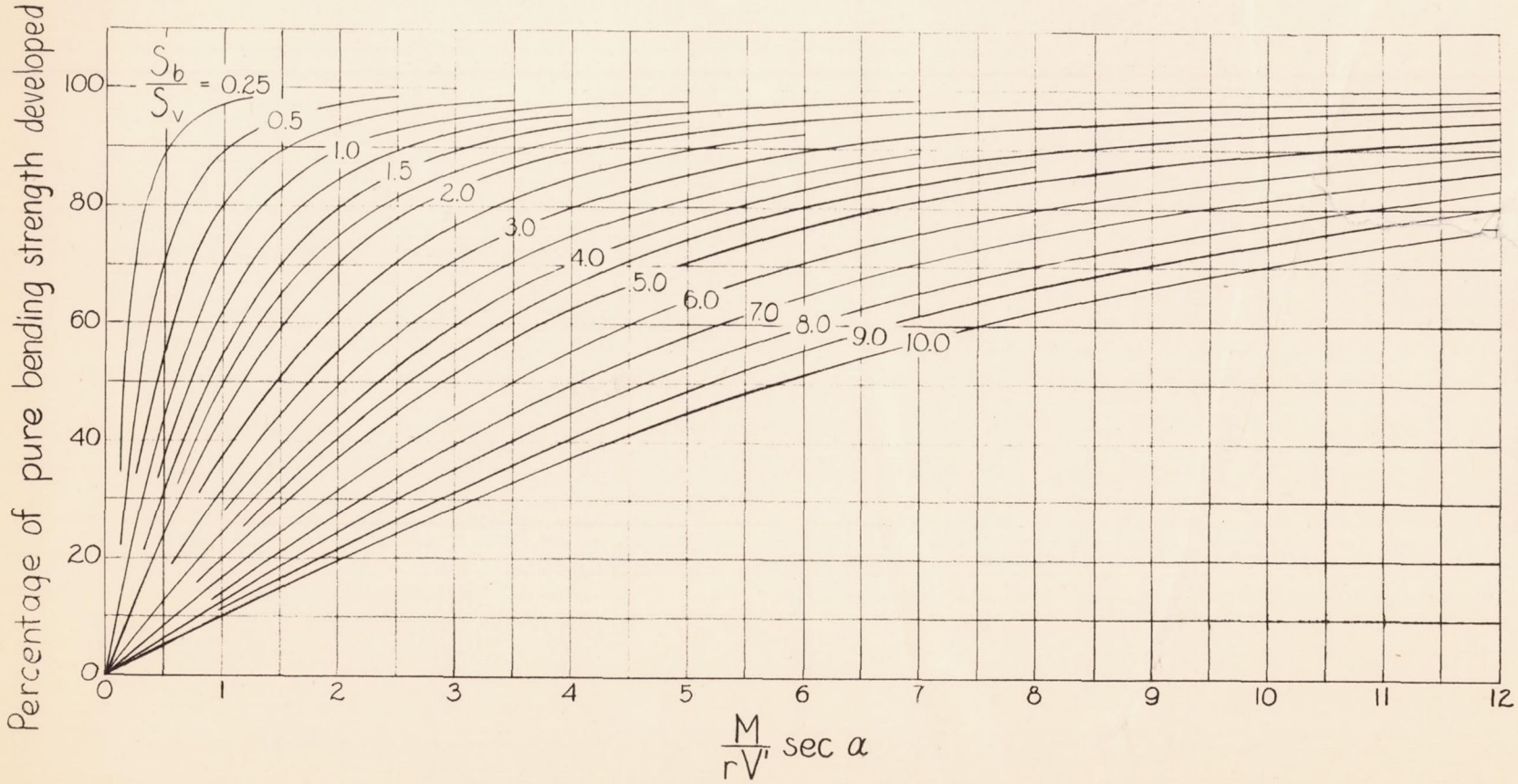

Figure 9.- Chart for bending strength of thin-walled truncated cones in combined transverse shear and bending. (See fig. 8, reference 4.)

24

L-442

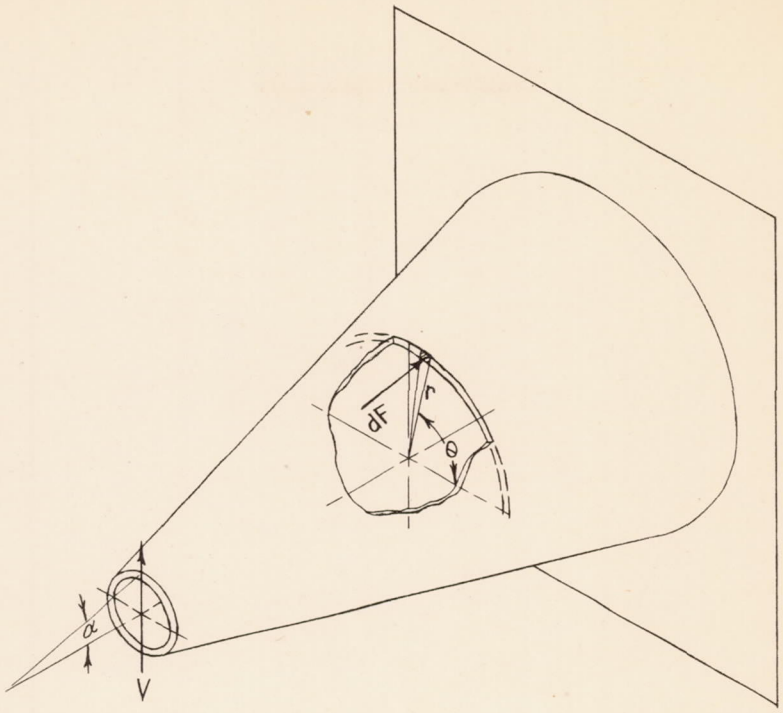

Figure 10.- Truncated cone subjected to combined transverse shear and bending.

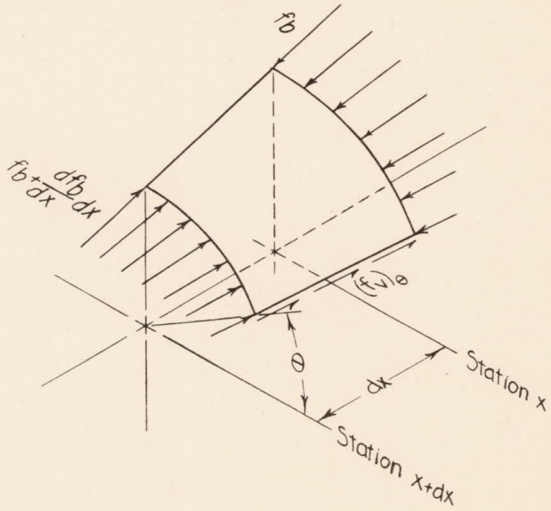

Figure 11.- Part element of a cone, showing longitudinal stresses due to shear and bending.

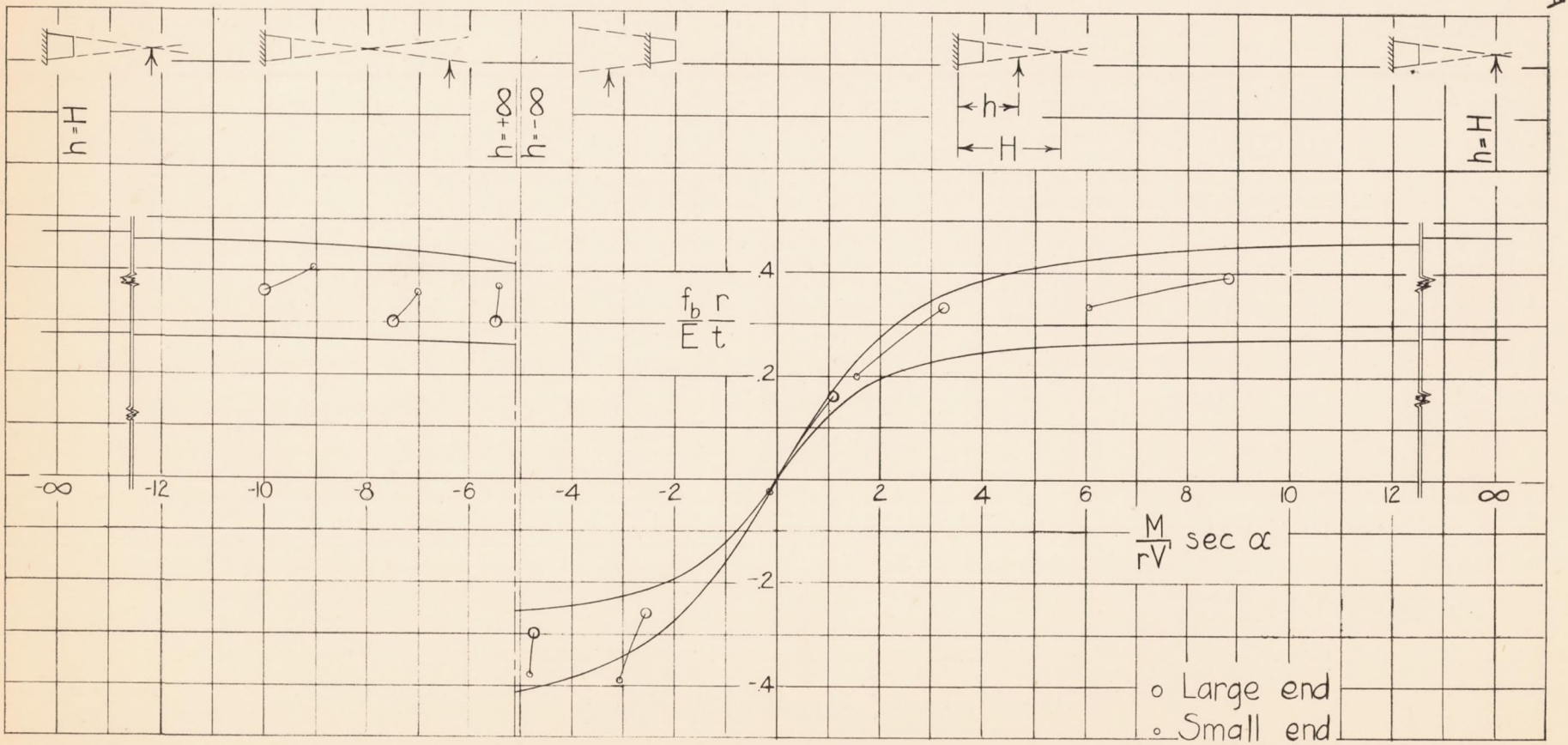

Figure 12.- Strength of thin-walled truncated cones in combined transverse shear and bending, for various positions of the resultant shear force.